Bull. Nov. Comp. Center, Comp. Science, 42 (2018), 23–28

Calculation of displacements around the crack formed during pulsed thermal load*

A.G. Maksimova, G.G. Lazareva, A.S. Arakcheev

Abstract. This paper presents the results of mathematical modeling of the problem of elasticity theory. The problem consists in the calculation of a model problem in a two-dimensional formulation aimed at finding the displacements around a crack.

Introduction

The objective of this paper is to numerically implement a new simplified elastic deformation model [1] to describe a crack propagating along a surface. Simplification of the model consists in reducing a system of differential equations of the theory of elasticity to the Fredholm integral equation of the second kind. This model may be used when calculating the conditions of forming cracks in metals under a strong thermal load. The existing models of cracking in the surface layer of a material at a pulsed thermal load are one-dimensional [2, 3].

1. Statement of the problem

We consider the problem of finding displacements around a crack at the surface of a rectangular sample. Let us assume that the crack is located along the axis x (Figure 1a). The equation for finding the displacements is the following [1]:

$$(1-2\nu)\Delta\boldsymbol{u} + \operatorname{grad}\operatorname{div}\boldsymbol{u} = 0.$$

where $\boldsymbol{u} = (u, v)$, ν is the Poisson ratio. We find the stationary solution of the system of equations of the elliptic type by finding the steady-state solution of the following evolutionary system of equations of the parabolic type in the Cartesian coordinates (y, z):

$$\begin{aligned}
(1-2\nu)\Big(\frac{\partial^2 u}{\partial y^2} + \frac{\partial^2 u}{\partial z^2}\Big) + \frac{\partial}{\partial y}\Big(\frac{\partial u}{\partial y} + \frac{\partial v}{\partial z}\Big) &= \frac{\partial u}{\partial \tau},\\
(1-2\nu)\Big(\frac{\partial^2 v}{\partial y^2} + \frac{\partial^2 v}{\partial z^2}\Big) + \frac{\partial}{\partial z}\Big(\frac{\partial u}{\partial y} + \frac{\partial v}{\partial z}\Big) &= \frac{\partial v}{\partial \tau},
\end{aligned} \tag{1}$$

*Experimental data and model development were supported by the Russian Science Foundation (project 17-79-20203). The reported study (computational experiment) was funded by the RFBR under the research project 18-31-00303.

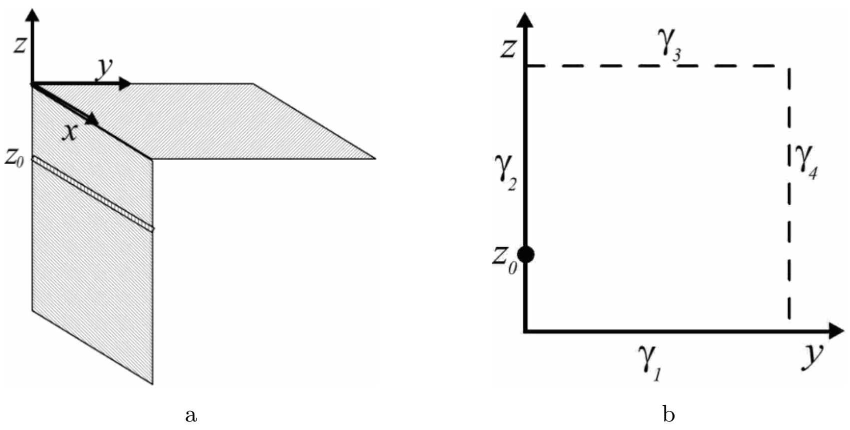

Figure 1. The coordinate system in the quarter space filled with an elastic medium (a) and the boundary of the computational domain (b)

where τ is the steady-state parameter. In the calculation domain (Figure 1b) let us set the location of a crack at a point z_0 on the axis z.

2. Boundary conditions

Let σ be the stress tensor with the components σ_{ij}, $f = (f_i) = (\sigma_{ij} n_j)$ are the surface forces, $i, j \in \{\text{“}y\text{”}, \text{“}z\text{”}\}$.

At the boundary γ_1, the condition $f|_{\gamma_1} = 0$ is satisfied (see Figure 1b). In terms of the stress tensor components: $\sigma_{yz}|_{\gamma_1} = 0$, $\sigma_{zz}|_{\gamma_1} = 0$.

At the boundary γ_2, the condition $f|_{\gamma_2} = \boldsymbol{n}_y \delta'(z - z_0)$ is satisfied, where $\boldsymbol{n}_y$ is the normal to γ_2, $\delta'(z)$ is the derivative of a Delta-like function. In terms of the stress tensor components: $\sigma_{yz}|_{\gamma_2} = 0$, $\sigma_{yy}|_{\gamma_2} = \delta'(z - z_0)$.

It is assumed that the boundaries γ_3 and γ_4 are far away from the crack. At these boundaries, the displacement is zero: $\boldsymbol{u}|_{\gamma_3} = \boldsymbol{u}|_{\gamma_4} = 0$.

The relation between the stresses and displacements is expressed by the Hooke law:

$$\sigma_{ij} = E\Big(\frac{1}{1+\nu} u_{ij} + \frac{\nu}{(1+\nu)(1-2\nu)} (u_{yy} + u_{zz})\delta_{ij}\Big),$$

where E is the Young modulus, $u_{ij} = \frac{1}{2}\Big(\frac{\partial u_i}{\partial x_j} + \frac{\partial u_j}{\partial x_i}\Big)$ is the strain tensor. Here $u_y := u$, $u_z := v$, $x_y := y$, $x_z := z$.

The Poisson ratio and the Young modulus fully characterize the elastic properties of the isotropic material.

Therefore, the boundary conditions on γ_1 can be written as

$$\frac{\partial u}{\partial z} + \frac{\partial v}{\partial y} = 0, \quad \nu \frac{\partial u}{\partial y} + (1-\nu)\frac{\partial v}{\partial z} = 0,$$

The boundary conditions on γ_2 are the following:

$$\frac{\partial u}{\partial z} + \frac{\partial v}{\partial y} = 0, \quad (1-\nu)\frac{\partial u}{\partial y} + \nu\frac{\partial v}{\partial z} = \frac{(1-2\nu)(1+\nu)}{E}\delta'(z-z_0).$$

The Delta function approximation based on the normalized Gauss function was chosen for the calculation. The choice is due to the results of the analysis [4]. Finally, we have

$$\delta(z) = \frac{1}{k\sqrt{\pi}}e^{-(\frac{z}{k})^2}, \quad \delta'(z) = -\frac{2z}{k^3\sqrt{\pi}}e^{-(\frac{z}{k})^2},$$

where k is the compression ratio.

3. Method of solution

We introduce in the calculation domain a uniform rectangular grid with the step h in y and z and denote by u_{ij}^n and v_{ij}^n the values of u and v at the node (y_i, z_j) at the nth iteration. The number of grid steps in y and z is N.

The numerical implementation is based on the Douglas–Rachford scheme and the run method [5]. The finite difference scheme for the system of equations (1) has the form:

$$\begin{aligned}
\frac{u_{ij}^{n+1/2} - u_{ij}^n}{\tau} &= (1-2\nu)(\Delta_y^{n+1/2}u + \Delta_z^n u) + \Delta_y^{n+1/2}u + \Delta_{yz}^n v,\\
\frac{u_{ij}^{n+1} - u_{ij}^{n+1/2}}{\tau} &= (1-2\nu)(\Delta_z^{n+1}u + \Delta_z^n u),\\
\frac{v_{ij}^{n+1/2} - v_{ij}^n}{\tau} &= (1-2\nu)(\Delta_y^n v + \Delta_z^{n+1/2}v) + \Delta_{yz}^n u + \Delta_z^{n+1/2}v,\\
\frac{v_{ij}^{n+1} - v_{ij}^{n+1/2}}{\tau} &= (1-2\nu)(\Delta_y^{n+1}v + \Delta_y^n v),
\end{aligned} \tag{2}$$

where

$$\Delta_y^n w = \frac{w_{i+1j}^n - 2w_{ij}^n + w_{i-1j}^n}{h^2}, \quad \Delta_z^n w = \frac{w_{ij+1}^n - 2w_{ij}^n + w_{ij-1}^n}{h^2},$$
$$\Delta_{yz}^n w = \frac{(w_{i+1j+1}^n - w_{i+1j-1}^n) - (w_{i-1j+1}^n - w_{i-1j-1}^n)}{4h^2}.$$

For the numerical implementation by the prediction method, the system of difference equations (2) is rewritten in the canonical form. Each equation is supplemented with the boundary conditions. Two equations for the y-components of the displacement u are:

$$
\begin{aligned}
&(2-2\nu)u_{i-1j}^{n+1/2} + \Big(4\nu - 4 - \frac{h^2}{\tau}\Big)u_{ij}^{n+1/2} + (2-2\nu)u_{i+1j}^{n+1/2} \\
&\qquad = (2\nu-1)u_{ij-1}^{n} + \Big(2 - 4\nu - \frac{h^2}{\tau}\Big)u_{ij}^{n} + (2\nu-1)u_{ij+1}^{n} - \\
&\qquad\quad \frac{1}{4}(v_{i+1j+1}^{n} - v_{i+1j-1}^{n} - v_{i-1j+1}^{n} + v_{i-1j-1}^{n}), \\
&u_{1j}^{n+1/2} - u_{2j}^{n+1/2} = \frac{\nu}{2(\nu-1)}(v_{2j-1}^{n} - v_{2j+1}^{n}) + \\
&\qquad\quad \frac{(1-2\nu)(1+\nu)}{(1-\nu)E}\frac{2h(jh-z_0)}{k^3\sqrt{\pi}}\exp\Big(-\frac{(jh-z_0)^2}{k^2}\Big), \\
&u_{Nj}^{n+1/2} = 0.
\end{aligned}
$$

$$
\begin{aligned}
&(1-2\nu)u_{ij-1}^{n+1} + \Big(4\nu - 2 - \frac{h^2}{\tau}\Big)u_{ij}^{n+1} + (1-2\nu)u_{ij+1}^{n+1} \\
&\qquad = -\frac{h^2}{\tau}u_{ij}^{n+1/2} + (1-2\nu)(u_{ij-1}^{n} - 2u_{ij}^{n} + u_{ij+1}^{n}), \\
&u_{i1}^{n+1} - u_{i2}^{n+1} = \frac{1}{2}(v_{i+12}^{n} - v_{i-12}^{n}), \\
&u_{iN}^{n+1} = 0.
\end{aligned}
$$

Two equations for the z-components of the displacement v are:

$$
\begin{aligned}
&(2-2\nu)v_{ij-1}^{n+1/2} + \Big(4\nu - 4 - \frac{h^2}{\tau}\Big)v_{ij}^{n+1/2} + (2-2\nu)v_{ij+1}^{n+1/2} \\
&\qquad = (2\nu-1)v_{i-1j}^{n} + \Big(2 - 4\nu - \frac{h^2}{\tau}\Big)v_{ij}^{n} + (2\nu-1)v_{i+1j}^{n} - \\
&\qquad\quad \frac{1}{4}(u_{i+1j+1}^{n} - u_{i+1j-1}^{n} - u_{i-1j+1}^{n} + u_{i-1j-1}^{n}), \\
&v_{i1}^{n+1/2} - v_{i2}^{n+1/2} = \frac{\nu}{2(\nu-1)}(u_{i-1,2}^{n} - u_{i+1,2}^{n}), \\
&v_{iN}^{n+1/2} = 0.
\end{aligned}
$$

$$
\begin{aligned}
&(1-2\nu)v_{i-1j}^{n+1} + \Big(4\nu - 2 - \frac{h^2}{\tau}\Big)v_{ij}^{n+1} + (1-2\nu)v_{i+1j}^{n+1} \\
&\qquad = -\frac{h^2}{\tau}v_{ij}^{n+1/2} + (1-2\nu)(v_{i-1j}^{n} - 2v_{ij}^{n} + v_{i+1j}^{n}), \\
&v_{1j}^{n+1} - v_{2j}^{n+1} = \frac{1}{2}(u_{2,j+1}^{n} - u_{2,j-1}^{n}), \\
&v_{Nj}^{n+1} = 0.
\end{aligned}
$$

4. Results of numerical calculations

In numerical calculations, the most indicative is the y-component of the displacement u, since the crack is located in the plane z. The Poisson ratio is equal to the ratio of the relative transverse compression to the relative longitudinal tension and characterizes the nature of the material from which the sample is made. The calculations were carried out on the grid with parameters $h = 0.01$, $t = 0.01$. The crack is located in the middle of the border. The data have been obtained after 50 iterations from the initial zero approximation.

Figure 2 presents the graphs of the displacement components at the boundary for different Poisson ratio values. Figure 3 shows the graphs of the displacement components in the whole computational domain. The numerical results obtained qualitatively correspond to the analytical solution from [1]. The difference is due to the approximation taken for the Delta function.

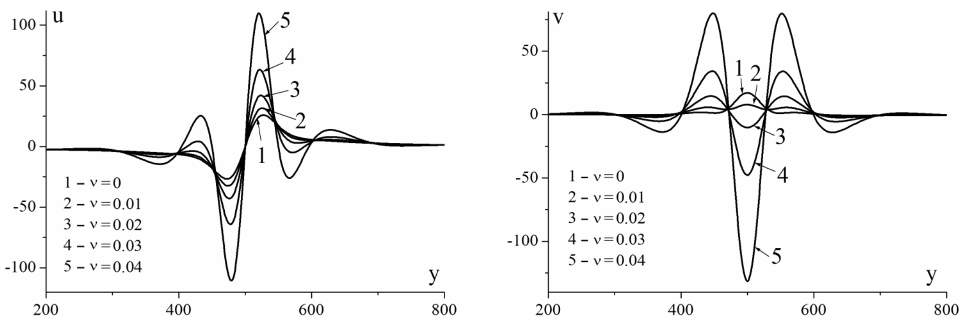

a b

Figure 2. Graphs of y-component (a) and z-component (b) of the displacement u at the boundary for different Poisson ratio values

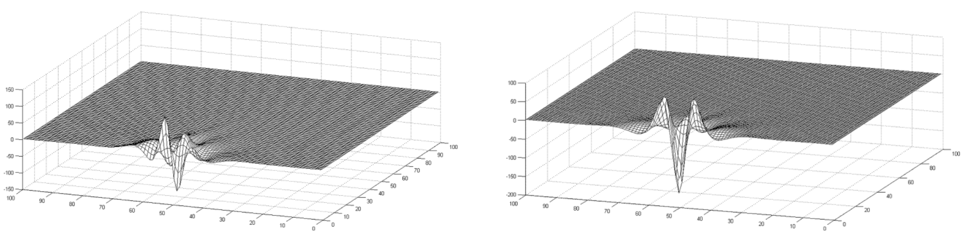

a b

Figure 3. Graphs of y-component (a) and z-component (b) of the displacement u in the whole computational domain for the Poisson ratio $\nu = 0.04$

Conclusion

A new simplified model of elastic deformations has been numerically implemented to describe the crack propagating along the surface. The model problem in two-dimensional statement has been solved. The values of the displacements around the crack for different Poisson ratios have been obtained. Further we suppose to use the model obtained for calculation of a condition of formation of cracks in metals at a strong thermal loading.

References

[1] Arakcheev A.S., Arakcheev S.A. Solution to force problem of linear elasticity theory for quarter space with edge-uniform forces // J. Applied and Theoretical Physics Research (to appear).

[2] Arakcheev A.S., Huber A., Wirtz M., et al. Theoretical investigation of crack formation in tungsten after heat loads // J. Nuclear Materials.—August 2015.—Vol. 463.—P. 246–249.

[3] Arakcheev A.S., Skovorodin D.I., Burdakov A.V., et al. Calculation of cracking under pulsed heat loads in tungsten manufactured according to ITER specifications // J. Nuclear Materials.—December 2015.—Vol. 467.—P. 165–171.

[4] Born M., Wolf E. Principles of Optics.—4th ed.—Pergamon Press, 1970.

[5] Yanenko N.N. Method of Fractional Steps for Solving Multidimensional Problems of Mathematical Physics.—Novosibirsk: Nauka. Siberian Division, 1967.

[6] Lazareva G.G., Arakcheev A.S., Kandaurov I.V., at al. Calculation of heat sink around cracks formed under pulsed heat load // J. Physics Conference Series.—2017.—Vol. 894.—012120. doi:10.1088/1742-6596/894/1/012120.

[7] Arakcheev A.S., Apushkinskaya D.E., Kandaurov I.V., at al. Two-dimensional numerical simulation of tungsten melting under pulsed electron beam // Fusion Engineering and Design (to appear).